

# Atmospheric pressure non-thermal plasma activation of CO<sub>2</sub> in a packed-bed dielectric barrier discharge reactor

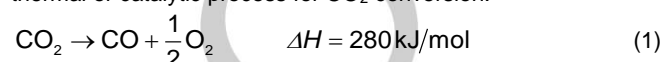
D.H. Mei, and X. Tu<sup>\*[a]</sup>

**Abstract:** Direct conversion of CO<sub>2</sub> into CO and O<sub>2</sub> was carried out in a packed-bed dielectric barrier discharge (DBD) non-thermal plasma reactor at low temperatures and atmospheric pressure. The maximum CO<sub>2</sub> conversion of 22.6% was achieved when BaTiO<sub>3</sub> pellets were fully packed into the discharge gap. The introduction of γ-Al<sub>2</sub>O<sub>3</sub> or 10 wt.% Ni/γ-Al<sub>2</sub>O<sub>3</sub> catalyst into the BaTiO<sub>3</sub> packed DBD reactor increased both CO<sub>2</sub> conversion and energy efficiency of the plasma process. Packing γ-Al<sub>2</sub>O<sub>3</sub> or 10 wt.% Ni/γ-Al<sub>2</sub>O<sub>3</sub> in the upstream of the BaTiO<sub>3</sub> bed showed higher CO<sub>2</sub> conversion and energy efficiency compared to that using middle or downstream packing modes as the reverse reaction of CO<sub>2</sub> conversion – the recombination of CO and O to form CO<sub>2</sub> is more likely to happen in the middle and downstream modes. Compared to the γ-Al<sub>2</sub>O<sub>3</sub> support, the coupling of the DBD with the Ni catalyst showed a higher CO<sub>2</sub> conversion which can be attributed to the presence of Ni active species on the catalyst surface. The argon plasma treatment of the reacted Ni catalyst provided extra evidence to confirm the role of Ni active species in the conversion of CO<sub>2</sub>.

## 1. Introduction

The increasing energy demand in the modern society has caused a large consumption of conventional carbon-containing fossil fuels, which consequently releases significant amounts of greenhouse gases (mainly CO<sub>2</sub>) into atmosphere. In 2013, the concentration of CO<sub>2</sub> in the atmosphere (~ 400 ppm) was 42% more than that of preindustrial level [1]. CO<sub>2</sub> has been considered as the main contributor to global warming and greenhouse effect, resulted in catastrophic effects to the ecosystem. The UK government has committed to reduce greenhouse gas emissions by at least 80% (from the 1990 baseline) by 2050 [2]. Different innovative and cost-effective technologies are being developed to tackle the global challenge of CO<sub>2</sub> emissions, such as reducing fossil fuel consumption, increasing the use of alternative and renewable energy, carbon capture and storage (CCS) and carbon capture and utilization (CCU). CCU is a promising approach to sustainably reduce carbon emissions, as in this process, the captured and separated CO<sub>2</sub> serves as a feedstock to produce a wide range of value-added synthetic fuels and platform chemicals (e.g. liquid fuels) [3]. Direct decomposition of CO<sub>2</sub> (Equation 1) is a typical CO<sub>2</sub> conversion route and has gained increasing attention as CO is a critical chemical feedstock for the synthesis

of liquid hydrocarbons, synthetic petroleum and oxygenates [4]. However, CO<sub>2</sub> is a highly stable and non-combustible molecule, considerable energy is thus required for upgrading and activation of CO<sub>2</sub>, which will induce high energy cost in the conventional thermal or catalytic process for CO<sub>2</sub> conversion.



Non-thermal plasma (NTP) technology provides a promising alternative solution for the conversion CO<sub>2</sub> into value-added fuels and chemicals at ambient conditions due to its distinct non-equilibrium character [5]. In non-thermal plasmas, the bulk gas temperature can be close to room temperature, while the generated electrons are highly energetic which collide with surrounding gas and produce a range of reactive species such as radicals, ions, excited atoms and molecules [6]. These energetic and reactive species can easily break most chemical bonds (e.g. C-O bonds) and enable thermodynamically unfavourable chemical reactions (e.g. CO<sub>2</sub> decomposition) to take place at ambient conditions in non-thermal plasmas. Various NTP systems have been used for the direct conversion of CO<sub>2</sub>, such as dielectric barrier discharge (DBD) [5a, 7], corona discharge [8], glow discharge [9], gliding arc discharge [10] and microwave discharge [11]. Recently, the use of packed bed DBD reactors for CO<sub>2</sub> conversion has attracted significant interest as the presence of catalytic or non-catalytic packing materials in the discharge can effectively intensify the local electric field near the contact points between the packing pellets and the average electric field in the plasma system, consequently enhances the process performance even using non-catalytic packing materials. The performance of a packed bed DBD reactor for chemical reaction is strongly dependent on the shape, size and physical and chemical properties (e.g. surface structure, adsorption capability and dielectric constant) of the packing materials [7m, 7n, 7p-r, 7t, 12]. Packing catalysts in a DBD reactor has great potential to enhance the performance of the plasma process due to the generation of both physical and catalytic effects of the catalysts on the reaction. Previous efforts were mainly devoted to investigating the effect of processing parameters (e.g. frequency, discharge power, dielectric materials, and feed flow rate, etc.) on the performance of plasma CO<sub>2</sub> processing in a packed bed DBD reactor [5a, 7c, 7d, 7h-j], while the knowledge of selecting a suitable catalyst which can be integrated into a DBD or packed bed DBD reactor for plasma CO<sub>2</sub> decomposition is largely unknown. Liu et al investigated CO<sub>2</sub> reduction to CO on different transition metal surfaces using a density function theory (DFT) method. They found that Ni surfaces are effective for CO<sub>2</sub> adsorption and decomposition in the reduction of CO<sub>2</sub> to CO [13]. Ni based catalysts have been used in plasma-catalytic CO<sub>2</sub> reforming of CH<sub>4</sub> and CO<sub>2</sub> hydrogenation [6a, 14], while limited efforts have been placed on the investigation of Ni catalysts in plasma CO<sub>2</sub> decomposition [12]. Catalysts can be placed in a DBD reactor in different ways. However, it is still not clear how the location of a catalyst bed in a DBD reactor affects

[a] Dr. D.H. Mei, Dr. X. Tu  
Department of Electrical Engineering and Electronics  
University of Liverpool  
Liverpool L69 3GJ  
UK  
Tel: +44-1517944513  
E-mail: xin.tu@liverpool.ac.uk

the performance of plasma chemical reactions, especially the CO<sub>2</sub> conversion process.

In this work, direct conversion of undiluted CO<sub>2</sub> into CO and O<sub>2</sub> was carried out in a packed-bed dielectric barrier discharge (DBD) at low temperatures. The effect of CO<sub>2</sub> flow rate and discharge power on the CO<sub>2</sub> conversion was evaluated in the DBD reactor packed with BaTiO<sub>3</sub> pellets only. An extra packing bed ( $\gamma$ -Al<sub>2</sub>O<sub>3</sub> or 10 wt.% Ni/ $\gamma$ -Al<sub>2</sub>O<sub>3</sub>) was placed in the different locations of the BaTiO<sub>3</sub> packed bed DBD reactor to understand the effect of different packing modes on the plasma conversion of CO<sub>2</sub>. The effect of plasma treatment on the performance of the Ni/ $\gamma$ -Al<sub>2</sub>O<sub>3</sub> catalyst in the CO<sub>2</sub> conversion process was also discussed.

## 2. Results and Discussion

### 2.1. Thermodynamic equilibrium analysis of CO<sub>2</sub> conversion process

The thermodynamic equilibrium calculation of CO<sub>2</sub> decomposition was carried out using the method based on minimization of Gibbs free energy in a closed system [15]. The details of this methodology can be found in previous literature [15a]. In the calculation, it was supposed that 1 mol of CO<sub>2</sub> was injected into the closed system. The final products include O<sub>2</sub> and CO which were identified as the only products in the experiment, while no ozone or carbon deposition was found. Figure 1 (a) shows the influence of reaction temperature and operating pressure on CO<sub>2</sub> conversion. Clearly, CO<sub>2</sub> begins to decompose near 2000 K with a low conversion of CO<sub>2</sub>. Extraordinarily high temperatures (2500–3000 K) are required to reach a CO<sub>2</sub> conversion of 20–40%, which leads to a high energy cost for the conversion of CO<sub>2</sub> using thermal processes. Increasing operating pressure significantly decreases the conversion of CO<sub>2</sub> at a constant reaction temperature. The thermal energy efficiency of CO<sub>2</sub> conversion was calculated using the method described in previous literature [16], as shown in Figure 1 (b). A maximum energy efficiency for CO<sub>2</sub> conversion can be achieved at an operating temperature between 2900 K and 3700 K. Increasing operating pressure would shift the maximum energy efficiency to a lower value at a higher temperature. As shown in Figure 1, decreasing operating pressure is beneficial for achieving both high CO<sub>2</sub> conversion and energy efficiency. However, vacuum systems are required if the conversion process is operated at low pressures (e.g. 0.1 atm), which will increase the operation cost.

### 2.2. CO<sub>2</sub> conversion in a BaTiO<sub>3</sub> packed-bed DBD reactor

Figure 2 shows the influence of discharge power and CO<sub>2</sub> flow rate on the conversion of CO<sub>2</sub> and energy efficiency in the BaTiO<sub>3</sub> packed-bed DBD reactor (reference mode). Clearly, increasing discharge power or decreasing CO<sub>2</sub> flow rate increased the conversion of CO<sub>2</sub>. The highest CO<sub>2</sub> conversion of 22.6% was obtained at the maximum discharge power of 40 W and a minimum CO<sub>2</sub> flow rate of 30 mL/min. Increasing the discharge power by changing the applied voltage at a fixed frequency can effectively increase the number of microdischarges generated in

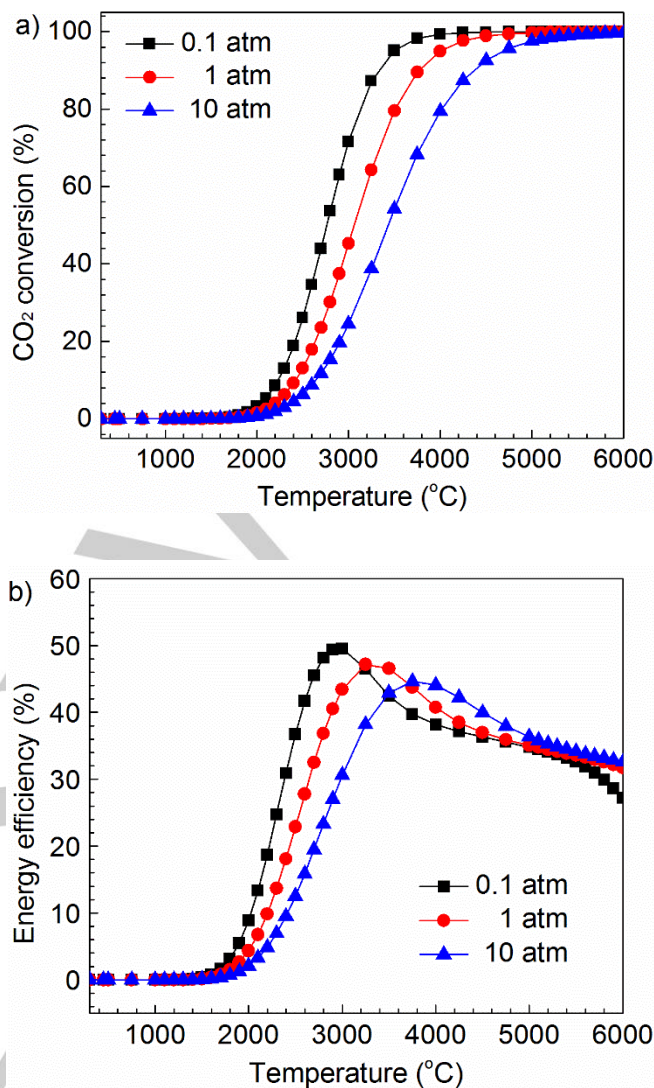


**Figure 1.** Thermodynamic equilibrium analysis of CO<sub>2</sub> conversion as a function of reaction temperature and operating pressure: a) CO<sub>2</sub> conversion; b) energy efficiency.

the DBD plasma, producing more chemical reaction channels and energetic species for CO<sub>2</sub> decomposition, and consequently enhanced the conversion of CO<sub>2</sub>. In addition, decreasing CO<sub>2</sub> flow while keeping other parameters constant increased the residence time of CO<sub>2</sub> in the discharge area and the possibility for CO<sub>2</sub> conversion through more collisions of CO<sub>2</sub> with energetic electrons and reactive species, resulted in the enhanced CO<sub>2</sub> conversion. Similar phenomenon was also reported in the plasma processing of CO<sub>2</sub> using a non-packed DBD reactor [17].

The effect of CO<sub>2</sub> gas flow and discharge power on the energy efficiency of the plasma process showed the opposite behavior. Increasing the CO<sub>2</sub> flow rate enhanced the energy efficiency of the plasma process although the conversion of CO<sub>2</sub> was lower at a higher CO<sub>2</sub> flow rate. In addition, the energy efficiency decreased by around 30% when increasing the discharge power from 20 to 40 W.



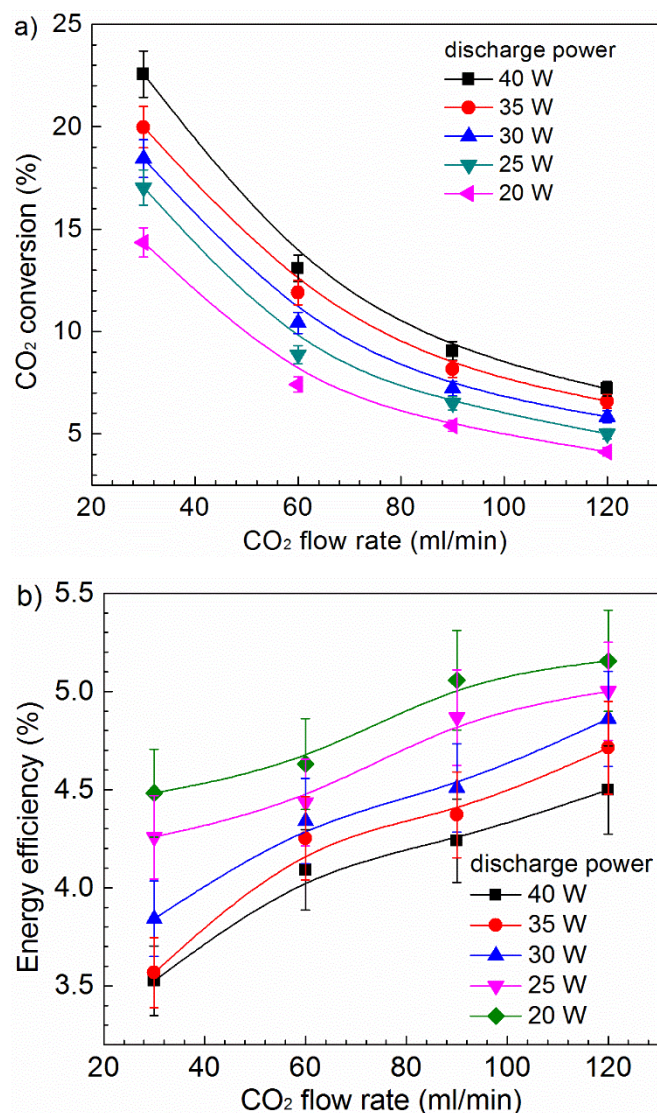


**Figure 2.** Effect of CO<sub>2</sub> flow rate and discharge power on a) CO<sub>2</sub> conversion and b) energy efficiency of the plasma process in the reference mode.

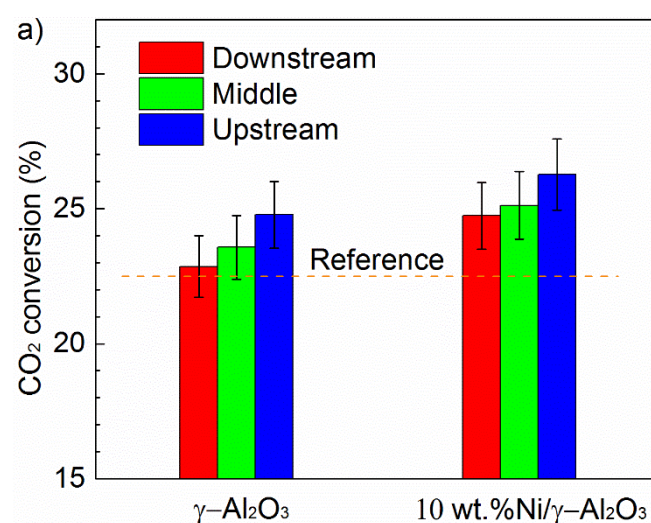
When the same experiment was carried out in the absence of the BaTiO<sub>3</sub> under similar operating conditions, a stable discharge could not be ignited in a pure CO<sub>2</sub> flow due to the presence of large discharge gap. This demonstrates that the presence of the packing material is vital for the process to take place under these experimental conditions. Previous results showed that the breakdown voltage of a CO<sub>2</sub> DBD was significantly decreased due to the reduced discharge gap when packing materials were fully packed in the discharge area [7p]. In addition, compared to the plasma conversion of CO<sub>2</sub> with no packing, the presence of the BaTiO<sub>3</sub> in the discharge can effectively enhance the CO<sub>2</sub> conversion [7p].

In the presence of packing materials, the discharge near the contact point between the packing pellets and between the pellets and the quartz wall was intensified, resulted in the enhanced electric field for chemical reactions. Our previous study found that

the average electric field in a CO<sub>2</sub> DBD reactor fully packed with the BaTiO<sub>3</sub> (1 mm) was almost two times of that in the CO<sub>2</sub> discharge with no packing [7p], which increased the mean electron energy and therefore significantly enhanced the conversion of CO<sub>2</sub>. Van Laer et al calculated the electric field distribution, electron temperature, and electron density in a DBD reactor packed with ZrO<sub>2</sub> beads by using a 2D fluid modeling [7q]. Their results showed that the local electric field near the contact points was stronger than that in the void (gas region). These findings can be ascribed to the accumulation of local charges of opposite sign at the contact point due to the polarization of the packing dielectric pellets by the applied potential difference between two electrodes. As a result, more highly energetic electrons could be generated for the conversion of CO<sub>2</sub> via electron impact dissociation [7q].

### 2.3. Effect of catalyst and different packing modes

Figure 3 shows the effect of  $\gamma$ -Al<sub>2</sub>O<sub>3</sub> support and Ni/ $\gamma$ -Al<sub>2</sub>O<sub>3</sub> catalyst on the conversion of CO<sub>2</sub> using different packing modes. Compared to the reaction using the BaTiO<sub>3</sub> only (reference mode), adding  $\gamma$ -Al<sub>2</sub>O<sub>3</sub> support or Ni/ $\gamma$ -Al<sub>2</sub>O<sub>3</sub> catalyst to the BaTiO<sub>3</sub> packed DBD reactor enhanced both the conversion of CO<sub>2</sub> and energy efficiency at the same discharge power.  $\gamma$ -Al<sub>2</sub>O<sub>3</sub> is a typical amphoteric oxide, on which an acidic gas (e.g. CO<sub>2</sub>) is preferably absorbed [7m]. The acid-basic property of  $\gamma$ -Al<sub>2</sub>O<sub>3</sub> facilitates the adsorption, activation and conversion of CO<sub>2</sub>. The positive effect of  $\gamma$ -Al<sub>2</sub>O<sub>3</sub> packing on CO<sub>2</sub> conversion was reported using a pulsed corona discharge reactor [18] and similar packed-bed DBD reactors [7m, 7i]. The presence of the Ni/ $\gamma$ -Al<sub>2</sub>O<sub>3</sub> catalyst in the discharge showed higher CO<sub>2</sub> conversion and energy efficiency compared to the same reaction over the  $\gamma$ -Al<sub>2</sub>O<sub>3</sub> support, which can be attributed to the existence of active Ni species over the catalyst surface which contributed to the dissociation of CO<sub>2</sub> molecules over the Ni catalyst [13a]. Interestingly, the position of the catalyst bed affected the reaction performance in terms of the CO<sub>2</sub> conversion and energy efficiency of the plasma process. The highest CO<sub>2</sub> conversions (24.7% for  $\gamma$ -Al<sub>2</sub>O<sub>3</sub> and 26.3% for Ni/ $\gamma$ -Al<sub>2</sub>O<sub>3</sub>) were obtained in the upstream mode.



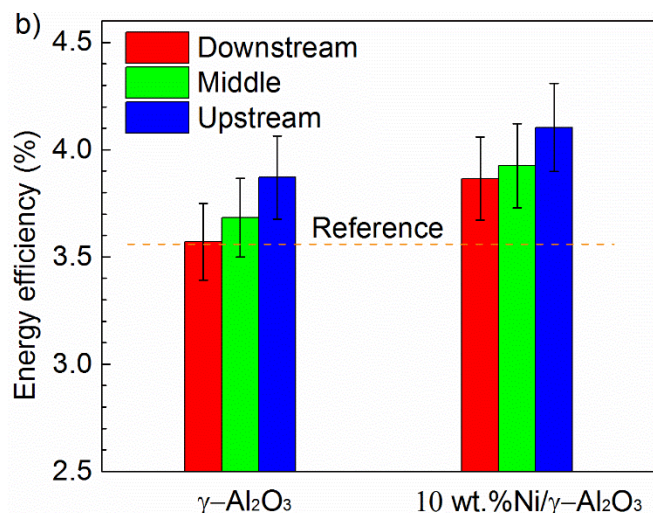


**Figure 3.** Effect of catalyst and support on a)  $\text{CO}_2$  conversion and b) energy efficiency using different packing modes (discharge power: 40 W;  $\text{CO}_2$  flow rate: 30 mL/min).

In this work,  $\text{CO}_2$  decomposition was also carried out in the same DBD reactor with a 15 cm length of  $\text{BaTiO}_3$  bed. The  $\text{CO}_2$  conversion and energy efficiency was 30.9% and 4.8%, respectively, which were higher than the values obtained using a  $\text{BaTiO}_3$  bed (12 cm) combined with an extra packing (3 cm,  $\gamma\text{-Al}_2\text{O}_3$  or  $\text{Ni}/\gamma\text{-Al}_2\text{O}_3$  catalyst) placed in the different locations of the DBD reactor at the same discharge power and flow rate. These results suggest that  $\text{BaTiO}_3$  is more effective for  $\text{CO}_2$  decomposition compared to the  $\gamma\text{-Al}_2\text{O}_3$  support and the  $\text{Ni}/\gamma\text{-Al}_2\text{O}_3$  catalyst in the plasma process. Our previous works showed the presence of  $\text{BaTiO}_3$  in a DBD reactor significantly enhanced the conversion of  $\text{CO}_2$  by around 250% which can be attributed to the physical effect (e.g. enhanced electric field) induced by the presence of  $\text{BaTiO}_3$  with a high dielectric constant and the dominant photocatalytic surface reactions driven by the plasma [19]. Thus, the present work will mainly focus on the investigation of the effect of the Ni catalyst and packing location on the plasma conversion of  $\text{CO}_2$ .

#### 2.4. Argon plasma treatment of Ni catalyst

After running the experiment for 2 hours, the reacted  $\text{Ni}/\gamma\text{-Al}_2\text{O}_3$  catalyst was treated by a pure Ar discharge for 30 min in the same DBD reactor at a discharge power of 40 W and an Ar flow rate of 50 mL/min. The plasma treated  $\text{Ni}/\gamma\text{-Al}_2\text{O}_3$  catalyst was then used for  $\text{CO}_2$  conversion in the same packed DBD reactor under the same experimental conditions as that used for testing the  $\text{Ni}/\gamma\text{-Al}_2\text{O}_3$  catalyst. Figure 4 shows the conversion of  $\text{CO}_2$  and energy efficiency using plasma treated and untreated  $\text{Ni}/\gamma\text{-Al}_2\text{O}_3$  catalyst. Clearly, compared to the  $\text{CO}_2$  conversion using the Ni catalyst, the use of the plasma treated spent Ni catalyst enhanced the  $\text{CO}_2$  conversion and energy efficiency in both middle and upstream packing modes. For instance, in the upstream packing mode, the  $\text{CO}_2$  conversion was increased by 8.5% when using the plasma

treated Ni catalyst, compared to that using the catalyst reacted for 2 hours.

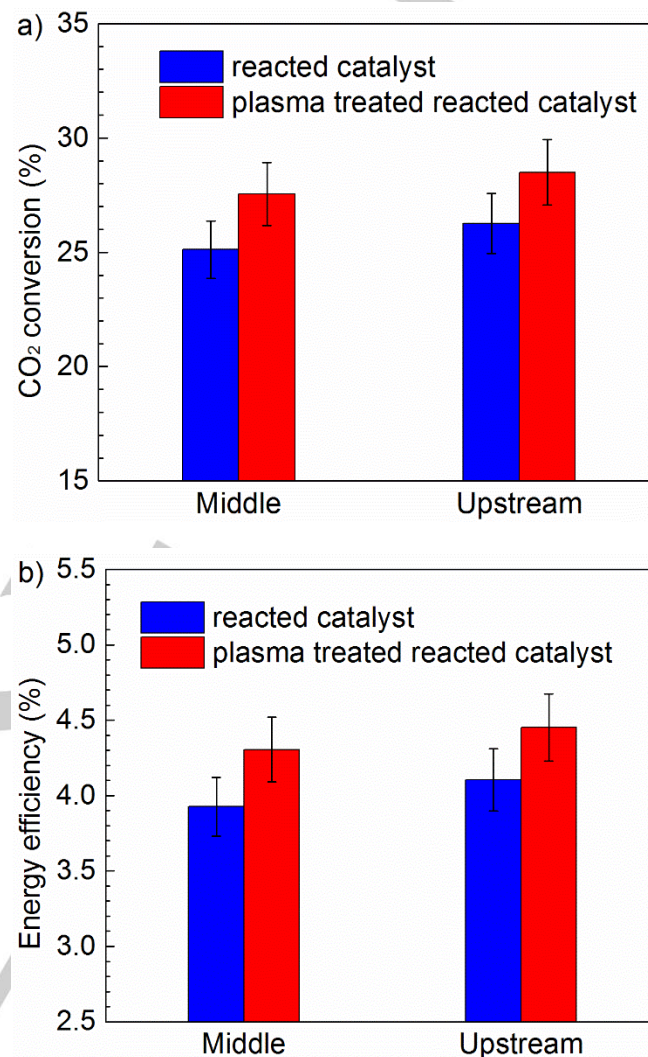


**Figure 4.** Effect of plasma treatment of the reacted  $\text{Ni}/\gamma\text{-Al}_2\text{O}_3$  catalyst on a)  $\text{CO}_2$  conversion and b) energy efficiency using different packing modes (discharge power: 40 W;  $\text{CO}_2$  flow rate: 30 mL/min).

#### 2.5. Discussion

Compared to the  $\text{CO}_2$  conversion using the  $\text{BaTiO}_3$  only (reference mode), adding  $\gamma\text{-Al}_2\text{O}_3$  support or  $\text{Ni}/\gamma\text{-Al}_2\text{O}_3$  catalyst to the  $\text{BaTiO}_3$  packed-bed DBD reactor enhanced the conversion of  $\text{CO}_2$  under the same operating conditions. Adding an extra packing bed ( $\gamma\text{-Al}_2\text{O}_3$  or  $\text{Ni}/\gamma\text{-Al}_2\text{O}_3$ ) in the discharge elongated the residence time of  $\text{CO}_2$  in the reaction zone although the power density of the reactor was decreased due to the increase of the discharge volume at the same discharge power. Clearly, the change of the residence time had a more prominent effect on the conversion of  $\text{CO}_2$ . One may argue that the increase of the bed length when using the extra  $\gamma\text{-Al}_2\text{O}_3$  or  $\text{Ni}/\gamma\text{-Al}_2\text{O}_3$  bed was the main factor that led to the enhanced  $\text{CO}_2$  conversion and energy



efficiency compared to those in the reference mode. The coupling of the DBD with the Ni/ $\gamma$ - $\text{Al}_2\text{O}_3$  catalyst showed higher  $\text{CO}_2$  conversion and energy efficiency compared to the same reaction over the  $\gamma$ - $\text{Al}_2\text{O}_3$  support regardless of the packing modes used, which indicates that the catalytic effect of Ni surfaces cannot be ruled out: dissociation of  $\text{CO}_2$  molecules over the Ni active sites on the surface of the catalyst [13a]. In the plasma  $\text{CO}_2$  conversion coupled with the Ni catalyst, both gas phase reactions and plasma-assisted surface reactions were contributed to the conversion of  $\text{CO}_2$ . In addition to the electron impact dissociation of  $\text{CO}_2$  (Equation 2) in the plasma gas phase,  $\text{CO}_2$  molecules in both ground and excited states can be absorbed onto the Ni surfaces to form  $\text{CO}_{2\text{ad}}$ , which will be dissociated into  $\text{CO}_{\text{ad}}$  and  $\text{O}_{\text{ad}}$  with the aid of energetic electrons (Equation 3). The  $\text{CO}_{\text{ad}}$  will be desorbed, releasing CO; while the  $\text{O}_{\text{ad}}$  will be recombined to  $\text{O}_{2\text{ad}}$  (Equation 4), followed by desorption to release  $\text{O}_2$ . The  $\text{CO}_{\text{ad}}$  and  $\text{O}_{\text{ad}}$  species can also be formed by adsorption of CO and O radicals from the gas phase onto the catalyst surface. The reverse reaction – the recombination of CO (or  $\text{CO}_{\text{ad}}$ ) and O (or  $\text{O}_{\text{ad}}$ ) to form  $\text{CO}_2$  (Equations 5 - 8) cannot be ruled out. However, it is reported that the recombination of O radicals to form  $\text{O}_2$  prevails over the recombination of CO with O radicals on the solid surfaces at low temperatures [12].



The results showed that the location of the packing bed ( $\gamma$ - $\text{Al}_2\text{O}_3$  or Ni/ $\gamma$ - $\text{Al}_2\text{O}_3$ ) played an important role in determining the reaction performance. Packing  $\gamma$ - $\text{Al}_2\text{O}_3$  or Ni/ $\gamma$ - $\text{Al}_2\text{O}_3$  in the upstream of the BaTiO<sub>3</sub> bed showed higher  $\text{CO}_2$  conversion compared to the same reaction using either middle or downstream packing mode. Note that the initial present reactant before entering the catalyst packing bed was different for different packing modes. For example,  $\text{CO}_2$  was the only initial reactant before the catalyst packing bed in the upstream mode, while in the middle and downstream modes, the initial reactants include CO,  $\text{O}_2$  and  $\text{CO}_2$ . The presence of the extra packing bed in the middle and downstream modes provided more chance for the recombination of CO and O to form  $\text{CO}_2$  through Equation 5 to 8, a competing reaction for  $\text{CO}_2$  decomposition in the plasma process. This could be the reason to get reduced  $\text{CO}_2$  conversion when placing the extra bed in the middle or downstream of the BaTiO<sub>3</sub> bed. In addition, Ni particles on the catalyst surface could be re-oxidized due to the formation of oxygen in the process, reducing the catalyst activity and thus the conversion of  $\text{CO}_2$ , especially for the middle and downstream modes.

The effect of the Ni active species on the  $\text{CO}_2$  conversion can also be evidenced from the argon plasma treatment of the reacted Ni catalyst. The plasma treated Ni catalysts showed higher  $\text{CO}_2$  conversion and energy efficiency compared to the reacted Ni catalyst used for 2 hours, which could be re-oxidized to form NiO due to the presence of oxygen. During the plasma reaction using

the fresh Ni/ $\gamma$ - $\text{Al}_2\text{O}_3$ , the Ni particle size might be decreased [12, 20]. The decrease in Ni particle size was beneficial to the re-utilization of the catalysts. In non-thermal plasmas, the gas kinetic temperature remains low (as low as room temperature), thus the thermal effect can be neglected in the plasma treatment process. In the argon plasma treatment of the Ni catalyst, highly energetic electrons and metastable argon species ( $\text{Ar}^*$ ) are considered as the key driving force to reduce metal oxide to metal on the catalyst surface [21]. The re-oxidized Ni/ $\gamma$ - $\text{Al}_2\text{O}_3$  catalyst could be reactivated through the argon plasma reduction process. In addition, the highly energetic electrons and metastable argon species ( $\text{Ar}^*$ ) in the plasma could affect the interactions between the Ni particles and  $\gamma$ - $\text{Al}_2\text{O}_3$ , and consequently enhance the distribution of Ni particles on the catalyst surface.

The energy efficiency of  $\text{CO}_2$  conversion using DBDs is relatively lower than that using microwave discharges or gliding arc plasmas. A maximum energy efficiency of 17.5% for  $\text{CO}_2$  conversion (42% conversion) was reported using a low pressure (10 Torr) microwave discharge combined with a NiO/TiO<sub>2</sub> catalyst [11b]. However, it is difficult to achieve such a high energy efficiency for  $\text{CO}_2$  conversion at atmospheric pressure, whilst low pressure systems are more complicated and costly. In atmospheric pressure gliding arc plasma systems, the high energy efficiency is generally obtained at the expense of a relatively low  $\text{CO}_2$  conversion. Indarto et al. reported a maximum energy efficiency of ~19% for  $\text{CO}_2$  conversion using a gliding arc discharge at a  $\text{CO}_2$  flow rate of 0.86 l/min, which corresponds to a relative low  $\text{CO}_2$  conversion (~15%) [10a].

DBD has the advantage of its flexibility and simplicity for coupling with appropriate catalysts, especially for the synthesis of value-added platform chemicals and synthetic fuels (e.g. oxygenates) from  $\text{CO}_2$  at ambient conditions. The combination of the plasma with the catalysts has great potential to generate plasma-catalytic synergy, which can further enhance the conversion and energy efficiency of the plasma process, especially breaking the trade-off barrier between the conversion and energy efficiency present in plasma chemical processes. The capability of scaling up for DBD reactors has been demonstrated in large scale plasma processes for water treatment, gas cleaning and ozone generation [22]. Therefore, DBD has the potential to be scaled-up for  $\text{CO}_2$  conversion and utilization. Significant efforts are required for the further investigation and optimization of the plasma  $\text{CO}_2$  conversion process through both experimental and modeling approaches [7h, 17, 23]. In addition, the integration of the plasma process with renewable energy sources (e.g. solar and wind energy) would provide a promising route of chemical energy storage for surplus electricity during the peak moment on the grid [24] and a sustainable alternative to reduce  $\text{CO}_2$  emission.

### 3. Conclusions

In this work, plasma decomposition of  $\text{CO}_2$  into CO and  $\text{O}_2$  was carried out in the BaTiO<sub>3</sub> packed-bed DBD reactor. Compared to the reaction using the BaTiO<sub>3</sub> only (reference mode), adding  $\gamma$ - $\text{Al}_2\text{O}_3$  or 10 wt.% Ni/ $\gamma$ - $\text{Al}_2\text{O}_3$  catalyst to the BaTiO<sub>3</sub> packed DBD reactor enhanced both  $\text{CO}_2$  conversion and energy efficiency of

the plasma process. The coupling of the discharge with the 10 wt.% Ni/ $\gamma$ - $\text{Al}_2\text{O}_3$  catalyst showed higher  $\text{CO}_2$  conversion and energy efficiency in comparison to that using  $\gamma$ - $\text{Al}_2\text{O}_3$  support. The results showed that the location of the catalyst bed played a key role in determining the process performance. Compared to the middle and downstream packing modes, placing an extra packing bed ( $\gamma$ - $\text{Al}_2\text{O}_3$  or Ni/ $\gamma$ - $\text{Al}_2\text{O}_3$ ) in the upstream of the  $\text{BaTiO}_3$  bed showed higher  $\text{CO}_2$  conversion and energy efficiency. Due to the presence of different reactant compositions before entering the extra packing bed using different packing modes, the recombination of CO and O to form  $\text{CO}_2$ , a reverse reaction for  $\text{CO}_2$  conversion, is more likely to happen on the catalyst or support surface in the middle and downstream modes, which leads to lower  $\text{CO}_2$  conversion against that obtained in the upstream packing mode. The results of the argon plasma treatment of the reacted Ni catalyst provided further evidence to support the role of the Ni active sites in the dissociation of  $\text{CO}_2$ , which showed the Ni/ $\gamma$ - $\text{Al}_2\text{O}_3$  catalyst had a higher  $\text{CO}_2$  conversion than that using  $\gamma$ - $\text{Al}_2\text{O}_3$ .

## Experimental Section

### Experimental setup

The experiments were carried out in a packed-bed DBD reactor, as shown in Figure 5 (a). An Al foil (ground electrode) was wrapped over a quartz tube with an external diameter of 25 mm and an inner diameter of 22 mm. A stainless-steel rod with an outer diameter of 6 mm was used as an inner electrode (high voltage electrode). As a result, the discharge gap was 8 mm in the absence of packing materials.

The DBD reactor was connected to an AC high voltage power supply with a peak-to-peak voltage of 10 kV and a fixed frequency of 50 Hz. All the electrical signals (applied voltage, current and voltage on the external capacitor) were recorded by a four-channel digital oscilloscope (TDS2014). The discharge power was calculated by using the Q-U Lissajous figure. A homemade online power measurement system was used to control the discharge power in real time. The discharge power can be adjusted by changing the applied voltage at a fixed frequency.

Three different packing materials  $\text{BaTiO}_3$  (TCU),  $\gamma$ - $\text{Al}_2\text{O}_3$  (Alfa Aesar) and 10 wt.% Ni/ $\gamma$ - $\text{Al}_2\text{O}_3$  with a diameter of 3 mm were evaluated in the plasma conversion of  $\text{CO}_2$ . The 10 wt.% Ni/ $\gamma$ - $\text{Al}_2\text{O}_3$  catalyst was prepared using the wetness impregnation method<sup>[14b]</sup>.  $\text{Ni}(\text{NO}_3)_2 \cdot 6\text{H}_2\text{O}$  (Alfa Aesar) was used as the metal precursor. Initially, the nickel nitrate was dissolved in the deionized water and stirred at room temperature for 1 h to obtain a 0.1 M solution. The appropriate weight of  $\gamma$ - $\text{Al}_2\text{O}_3$  (3 mm diameter beads) was added to the metal precursor solution and impregnated for 12 h. After that, the solution containing  $\gamma$ - $\text{Al}_2\text{O}_3$  beads was evaporated at 80 °C for 4 h and dried at 110 °C overnight, followed by the calcination at 400 °C for 4 h. Prior to the plasma reaction, the Ni catalyst was reduced in an Ar- $\text{H}_2$  plasma for 30 mins at a discharge power of 40 W and a total flow rate of 50 mL/min with 20 vol.%  $\text{H}_2$  in the same DBD reactor. Previous work demonstrated that NiO can be reduced to Ni on the

catalyst surface using a similar Ar/ $\text{H}_2$  DBD<sup>[25]</sup>. In addition, the  $\gamma$ - $\text{Al}_2\text{O}_3$  pellets were dried at 110 °C overnight to remove moistures before the plasma reaction.

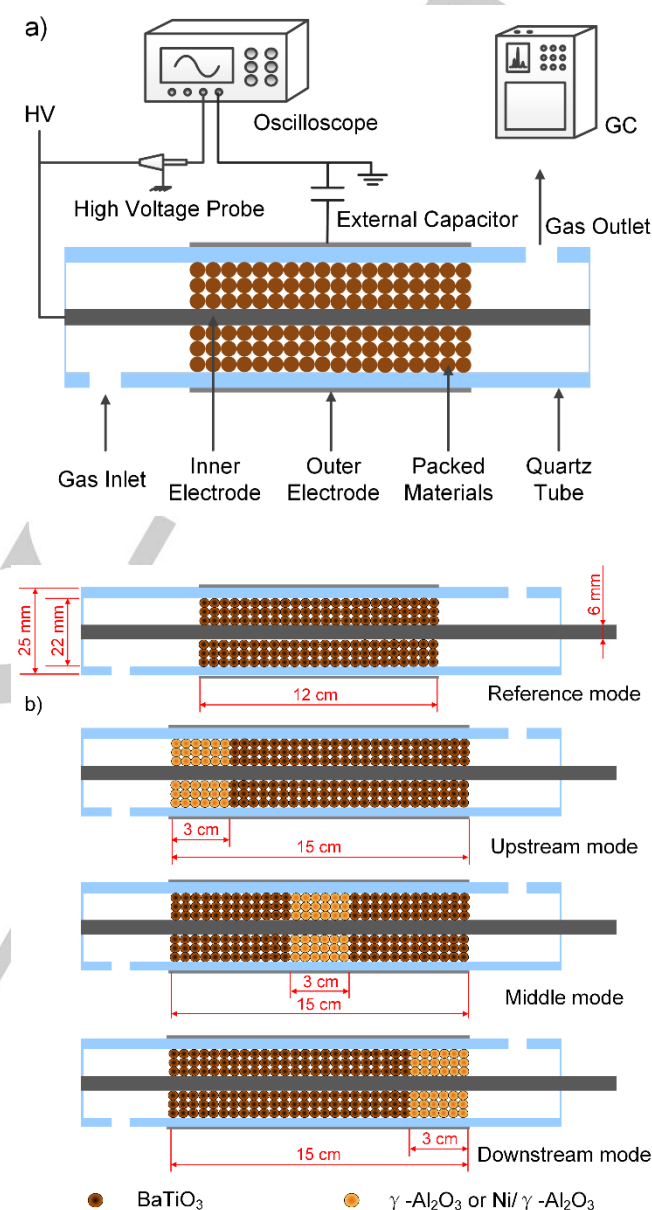


**Figure 5.** Schematic diagram of a) the experimental setup and b) different packing modes.

Different packing modes were used to understand the effect of the location of catalyst bed on the plasma conversion of  $\text{CO}_2$ , as shown in Figure 1 (b). In the reference mode, only  $\text{BaTiO}_3$  pellets were fully packed into the discharge area with a discharge length of 120 mm, while  $\gamma$ - $\text{Al}_2\text{O}_3$  (or Ni/ $\gamma$ - $\text{Al}_2\text{O}_3$ ) packing bed can be placed in the upstream, middle and downstream of the  $\text{BaTiO}_3$  bed, forming three different packing modes: upstream mode, middle mode and downstream mode, respectively. The length of

the  $\gamma$ -Al<sub>2</sub>O<sub>3</sub> (or Ni/ $\gamma$ -Al<sub>2</sub>O<sub>3</sub>) bed was 30 mm, while the length of the discharge was 150 mm in these three packing modes.

### Gas analysis and parameter definition

The gas products were analyzed by a two-channel gas chromatography (GC, Shimadzu GC2014) equipped with a thermal conductivity detector (TCD) and a flame ionization detector (FID) and. Each measurement was repeated three times when the reaction reached to a steady state. In this work, ozone and carbon deposition were not detected. The conversion of CO<sub>2</sub> (C), CO selectivity (S) and the energy efficiency of the plasma process ( $\eta$ ) were determined by Equations 9 to 11, respectively:

$$C_{\text{CO}_2}(\%) = \frac{\text{CO}_2 \text{ converted (mol/s)}}{\text{CO}_2 \text{ introduced (mol/s)}} \times 100 \quad (9)$$

$$S_{\text{CO}}(\%) = \frac{\text{CO produced (mol/s)}}{\text{CO}_2 \text{ converted (mol/s)}} \times 100 \quad (10)$$

$$\eta(\%) = \frac{\text{CO}_2 \text{ flow rate (ml/s)} \cdot C_{\text{CO}_2}(\%) \cdot \Delta H(\text{kJ/mol})}{22.4 \times \text{Discharge power (W)}} \quad (11)$$

The CO selectivity is close to 1, which suggests the CO is the major carbon containing product in the plasma conversion.

### Acknowledgements

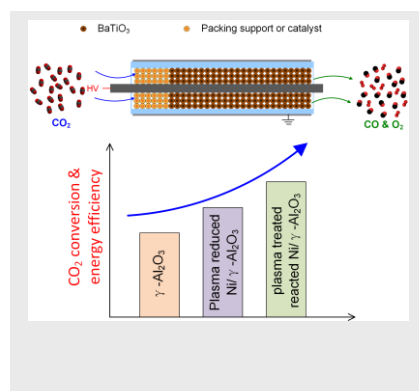
The financial support of this work by the EPSRC SUPERGEN Hydrogen & Fuel Cell (H2FC) Programme (Ref. EACPR\_PS5768) and the EPSRC CO2Chem Seedcorn grant is gratefully acknowledged.

**Keywords:** plasma-catalysis • non-thermal plasma • dielectric barrier discharge • packed-bed • CO<sub>2</sub> conversion

- [1] The State of Greenhouse Gases in the Atmosphere Based on Global Observations through 2013, *World Meteorological Organization*, **2014**, pp.1-10.
- [2] EurObserv'ER Biogas barometer, **2012**.
- [3] aE. V. Kondratenko, G. Mul, J. Baltrusaitis, G. O. Larrazabal, J. Perez-Ramirez, *Energy Environ. Sci.* **2013**, 6, 3112-3135; bM. Mikkelsen, M. Jorgensen, F. C. Krebs, *Energy Environ. Sci.* **2010**, 3, 43-81.
- [4] J. Medina-Ramos, R. C. Pupillo, T. P. Keane, J. L. DiMeglio, J. Rosenthal, *J. Am. Chem. Soc.* **2015**, 137, 5021-5027.
- [5] aS. Paulussen, B. Verheyde, X. Tu, C. De Bie, T. Martens, D. Petrovic, A. Bogaerts, B. Sels, *Plasma Sources Sci. Technol.* **2010**, 19, 034015; bS. Mahammadunnisa, E. L. Reddy, D. Ray, C. Subrahmanyam, J. C. Whitehead, *Int. J. Greenhouse Gas Control* **2013**, 16, 361-363.
- [6] aX. Tu, J. C. Whitehead, *Appl. Catal. B-Environ* **2012**, 125, 439-448; bW. Wang, B. Patil, S. Heijckers, V. Hessel, A. Bogaerts, *ChemSusChem* **2017**, 10, 2145-2157.
- [7] aR. Aerts, R. Snoeckx, A. Bogaerts, *Plasma Process. Polym.* **2014**, 11, 985-992; bF. Brehmer, S. Weizel, M. C. M. van de Sanden, R. Engeln, *J. Appl. Phys.* **2014**, 116, 123303; cR. Aerts, W. Somers, A. Bogaerts, *ChemSusChem* **2015**, 8, 702-716; dX. Duan, Y. Li, W. Ge, B. Wang, *Greenh. Gases* **2015**, 5, 131-140; eM. Ramakers, I. Michielsens, R. Aerts, V. Meynen, A. Bogaerts, *Plasma Process. Polym.* **2015**, 12, 755-763; fI. Belov, S. Paulussen, A. Bogaerts, *Plasma Sources Sci. Technol.* **2016**, 25, 015023; gI. Belov, J. Vanneste, M. Aghaee, S. Paulussen, A. Bogaerts, *Plasma Process. Polym.* **2016**; hD. Mei, Y.-L. He, S. Liu, J. Yan, X. Tu, *Plasma Process. Polym.* **2016**, 13, 544-556; iA. Ozkan, T. Dufour, A. Bogaerts, F. Reniers, *Plasma Sources Sci. Technol.* **2016**, 25, 045016; jA. Ozkan, T. Dufour, T. Silva, N. Britun, R. Snyders, A. Bogaerts, F. Reniers, *Plasma Sources Sci. Technol.* **2016**, 25, 025013; kR. X. Li, Q. Tang, S. Yin, T. Sato, *Appl. Phys. Lett.* **2007**, 90, 131502; lS. Wang, Y. Zhang, X. Liu, X. Wang, *Plasma Chem. Plasma Process.* **2012**, 32, 979-989; mQ. Q. Yu, M. Kong, T. Liu, J. H. Fei, X. M. Zheng, *Plasma Chem. Plasma Process.* **2012**, 32, 153-163; nM. A. Lindon, E. E. Scime, *Frontiers in Physics* **2014**, 2, article 55; oX. F. Duan, Z. Y. Hu, Y. P. Li, B. W. Wang, *AIChE J* **2015**, 61, 898-903; pD. H. Mei, X. B. Zhu, Y. L. He, J. D. Yan, X. Tu, *Plasma Sources Sci. Technol.* **2015**, 24, 015011; qK. Van Laer, A. Bogaerts, *Energy Technol.* **2015**, 1038-1044; rT. Butterworth, R. Elder, R. Allen, *Chem. Eng. J.* **2016**, 293, 55-67; sX. Zhu, X. Tu, D. Mei, C. Zheng, J. Zhou, X. Gao, Z. Luo, M. Ni, K. Cen, *Chemosphere* **2016**, 155, 9-17; tD. Ray, C. Subrahmanyam, *RSC Adv.* **2016**, 6, 39492-39499.
- [8] aW. Xu, M. W. Li, G. H. Xu, Y. L. Tian, *Jpn. J. Appl. Phys.* **2004**, 43, 8310-8311; bG. Horvath, J. D. Skalny, N. J. Mason, *J. Phys. D Appl. Phys.* **2008**, 41, 225207.
- [9] aP. G. Reyes, E. F. Mendez, D. Osorio-Gonzalez, F. Castillo, H. Martinez, *Phys. Status. Solidi. C* **2008**, 5, 907-910; bS. L. Brock, T. Shimojo, M. Marquez, C. Marun, S. L. Suib, H. Matsumoto, Y. Hayashi, *J. Catal.* **1999**, 184, 123-133.
- [10] aA. Indarto, D. R. Yang, J. W. Choi, H. Lee, H. K. Song, *J. Hazard. Mater.* **2007**, 146, 309-315; bS. C. Kim, M. S. Lim, Y. N. Chun, *Plasma Chem. Plasma Process.* **2014**, 34, 125-143; cT. G. Nunnally, K.; Rabinovich, A.; Fridman, A.; Gutsol, A.; Kemoun, A., *J. Phys. D Appl. Phys.* **2011**, 44, 274009; dM. Ramakers, G. Trenchev, S. Heijckers, W. Wang, A. Bogaerts, *ChemSusChem* **2017**, 10, 2642-2652.
- [11] aH. S. Uhm, H. S. Kwak, Y. C. Hong, *Environ. Pollut.* **2016**, 211, 191-197; bG. Chen, V. Georgieva, T. Godfroid, R. Snyders, M.-P. Delplancke-Ogletree, *Appl. Catal. B: Environ.* **2016**, 190, 115-124.
- [12] K. Zhang, G. Zhang, X. Liu, A. N. Phan, K. Luo, *Ind. Eng. Chem. Res.* **2017**, 56, 3204-3216.
- [13] aS. G. Wang, D. B. Cao, Y. W. Li, J. Wang, H. Jiao, *J. Phys. Chem. B* **2005**, 109, 18956-18963; bC. Liu, T. R. Cundari, A. K. Wilson, *The J. Phys. Chem. C* **2012**, 116, 5681-5688.
- [14] aY. Zeng, X. Tu, *J. Phys. D: Appl. Phys.* **2017**, 50, 184004; bD. Mei, B. Ashford, Y.-L. He, X. Tu, *Plasma Process. Polym.* **2017**, 14, e1600076.
- [15] aM. K. Nikoo, N. A. S. Amin, *Fuel Process. Technol.* **2011**, 92, 678-691; bW. Wang, M. Rong, Y. Wu, J. D. Yan, *J. Phys. D: Appl. Phys.* **2014**, 47, 255201; cW. Wang, A. Bogaerts, *Plasma Sources Sci. Technol.* **2016**, 25, 055025.
- [16] W. Wang, D. Mei, X. Tu, A. Bogaerts, *Chem. Eng. J.* **2017**, 330, 11-25.
- [17] D. Mei, X. Tu, *J. CO<sub>2</sub> Util.* **2017**, 19, 68-78.
- [18] Y. Z. Wen, X. Z. Jiang, *Plasma Chem. Plasma Process.* **2001**, 21, 665-678.
- [19] D. Mei, X. Zhu, C. Wu, B. Ashford, P. T. Williams, X. Tu, *Appl. Catal. B: Environ.* **2016**, 182, 525-532.
- [20] E. Jwa, S. B. Lee, H. W. Lee, Y. S. Mok, *Fuel Process. Technol.* **2013**, 108, 89-93.
- [21] aC. J. Liu, J. J. Zou, K. L. Yu, D. G. Cheng, Y. Han, J. Zhan, C. Ratanatawanate, B. W. L. Jang, *Pure Appl. Chem.* **2006**, 78, 1227-1238; bC. J. Liu, M. Y. Li, J. Q. Wang, X. T. Zhou, Q. T. Guo, J. M. Yan, Y. Z. Li, *Chin. J. Catal.* **2016**, 37, 340-348.
- [22] aT. Nozaki, K. Okazaki, *Green Process. Syn.* **2012**, 1, 517-523; bH. L. Chen, H. M. Lee, S. H. Chen, M. B. Chang, *Ind. Eng. Chem. Res.* **2008**, 47, 2122-2130; cA. Mizuno, *Catal. Today* **2013**, 211, 2-8.
- [23] R. Aerts, T. Martens, A. Bogaerts, *J. Phys. Chem. C* **2012**, 116, 23257-23273.
- [24] R. Snoeckx, Y. X. Zeng, X. Tu, A. Bogaerts, *RSC Adv.* **2015**, 5, 29799-29808.
- [25] X. Tu, H. J. Gallon, J. C. Whitehead, *Catal. Today* **2013**, 211, 120-125.

## ARTICLE

The location of the catalyst bed in the packed-bed DBD reactor plays a crucial role in determining the performance of the plasma  $\text{CO}_2$  conversion. Argon plasma treatment of the reacted Ni catalyst showed higher  $\text{CO}_2$  conversion compared to untreated catalyst.



Danhua Mei, and Xin Tu\*

Page No. – Page No.

Atmospheric pressure non-thermal plasma activation of  $\text{CO}_2$  in a packed-bed dielectric barrier discharge reactor